Melatonin ameliorates acute lung injury caused by paraquat poisoning by promoting PINK1 and BNIP3 expression

Yiyuan Yin
Department of Emergency Medicine, ShengJing Hospital of China Medical University, Shenyang, China
Haitao Shen (shenht@sj-hospital.org)
Department of Emergency Medicine, ShengJing Hospital of China Medical University, Shenyang, China

Research Article

Keywords: melatonin, mitophagy, mitochondrial DNA, paraquat poisoning, acute lung injury

Posted Date: February 7th, 2023

DOI: https://doi.org/10.21203/rs.3.rs-2542577/v1

Abstract

Paraquat (PQ) poisoning can result in multiple organ dysfunction syndrome, mainly manifesting as acute lung injury and acute respiratory distress syndrome. No specific cure exists for PQ poisoning. However, by scavenging mitochondrial DNA (mtDNA), the damage-associated molecular pattern during PQ poisoning, mitophagy can ameliorate the downstream inflammatory pathways activated by mtDNA. Melatonin (MT), however, can promote the expression of PINK1 and BNIP3, which are key proteins involved in mitophagy. In this study, we first explored whether MT could reduce PQ-induced acute lung injury by affecting mitophagy in animal models, and then, we studied the specific mechanism associated with this process through in vitro experiments. We also evaluated MT intervention in the PQ group, while inhibiting the expression of PINK1 and BNIP3, to further determine whether the protective effects of MT are associated with its effect on mitophagy. We found that when the expression of PINK1 and BNIP3 was inhibited, MT intervention could not reduce mtDNA leakage and the release of inflammatory factors caused by PQ exposure, suggesting that the protective effect of MT was mitigated. These results suggest that by promoting the expression of PINK1 and BNIP3 and activating mitophagy, MT can reduce mtDNA/TLR9-mediated acute lung injury during PQ poisoning. The results of this study could provide guidance for the clinical treatment of PQ poisoning to reduce associated mortality.

1 Introduction

Paraquat (PQ) is a widely used herbicide and is highly toxic. After entering the human body through skin exposure or through the mouth and nose, it first and mainly damages the lungs, leading to acute lung injury and acute respiratory distress syndrome, which can ultimately result in multiple organ dysfunction syndrome. The mortality rate of PQ poisoning is extremely high, with no effective treatment available at present [1, 2]. Since PQ is structurally similar to polyamines, after it enters the human body, alveolar cells will actively transport it to alveolar epithelial cells through the polyamine transport system. PQ mainly acts on the mitochondrial electron transport chain. As a non-specific high-energy electron acceptor and donor, it disrupts the mitochondrial electron transport chain in a cyclic manner; PQ first steals electrons and then transports them to molecular oxygen, producing toxic reactive oxygen species [3–5]. Reduced PQ is a free radical that can provide an electron to oxygen to generate the powerful superoxide radical. The superoxide radical can then form more toxic substances, which in turn damage mitochondria and other cellular structures [6, 7]. After disruption of the mitochondrial structure, mitochondrial DNA (mtDNA) leakage into the cytoplasm can occur. As fully unmethylated DNA, the leaked mtDNA probably leads to TLR9 activation, which in turn activates downstream inflammatory pathways, causes the release of TNF-α and IL-1β, and ultimately results in lung injury [8–10]. Mitophagy, as an important mechanism of mitochondrial quality control [11, 12], can remove damaged mitochondria, reduce the leakage of mtDNA, and maintain stability of the body through three pathways, namely the PINK1/Parkin, BNIP3/NIX, and FUNDC1 pathways. Melatonin (MT), also known as the pineal hormone, is a hormone secreted by the pineal gland of the brain. MT is an indole derivative, and its chemical name is N-acetyl-5-methoxytryptamine. MT has strong neuroendocrine immunomodulatory activity and can scavenge free

radicals to confer resistance to oxidation [13–16]. Studies have shown that by promoting the expression of PINK1 and BNIP3, MT can induce mitophagy and reduce the inflammatory response in the body [17–19]. Therefore, we speculated that by activating PINK1 and BNIP3, MT can activate mitophagy, reduce mtDNA leakage caused by PQ exposure, and consequently reduce acute lung injury mediated by TLR9 and downstream inflammatory pathways. In this study, through H&E staining and immunofluorescence, we first observed that compared with that in mice in the PQ group, lung injury after MT intervention was reduced, the expression of PINK1 and BNIP3 was increased, and the expression level of the inflammatory protein TLR9 was decreased; by using electron microscopy, we also observed an increase in the number of autophagosomes. These results suggest that MT has a protective effect on PQ-induced acute lung injury, which is closely related to the activation of mitophagy. Using A549 cells as an in vitro model, we then observed that mtDNA leakage led to TLR9 hyperactivation; after MT intervention, the expression of PINK1 and BNIP3 was increased and the levels of inflammatory factors were decreased. These findings validate the protective effect of MT and the associated mechanism related to mitophagy. To further verify that PINK1 and BNIP3 are the key proteins involved in the protective effect of MT, we evaluated MT intervention in the PQ group after inhibiting the expression of PINK1 and BNIP3 in vitro. We found that the release of inflammatory factors due to PQ exposure was not reduced upon MT intervention and was even increased, indicating that the protective effect of MT was mitigated, which further confirmed our conjecture. This study aimed to investigate the role of mitophagy in the mtDNA/TLR9 inflammatory pathway and its protective mechanism with respect to PQ poisoning-induced acute lung injury, to provide guidance for the clinical treatment of this condition.

2 Materials And Methods

2.1 In vivo study

2.1.1 Animals

Specific-pathogen-free male C57BL/6J mice (6–8weeks-old, with a body weight of 20–25 g; n = 32) were purchased from Beijing HFK Biotechnology Co., Ltd. and were maintained in the laboratory of the experimental animal center of Shengjing Hospital of China Medical University for 1 week such that the mice were able to adapt to the new environment. All mice had continuous access to water and food ad libitum. Experimental animals were maintained in a room with a controlled temperature (20–25°C) and constant humidity (40–70%), and a natural photoperiod (12/12 h light/dark cycle) was used. This experiment was approved by the Ethics Committee of Shengjing Hospital of China Medical University (No. 2021PS526K).

2.1.2 Establishment of model and grouping of animals

Mice were randomly assigned to four groups (n = 8), namely the control group (Group A), PQ group (Group B), MT + PQ group (Group C), and MT group (Group D). Groups B and C were first intraperitoneally injected with PQ (Sigma, 36541) at 30 mg/kg, and Groups A and D were intraperitoneally injected with the

same volume of normal saline. One hour later, mice in Groups C and D were intraperitoneally injected with MT (Sigma, M5250) at 20 mg/kg, whereas those of Groups A and B were intraperitoneally injected with the same volume of normal saline. Twenty-four hours later, mice in Groups C and D were intraperitoneally injected with MT at 20 mg/kg, and those of Groups A and B were intraperitoneally injected with the same volume of normal saline .

2.1.3 Collection and storage of samples

After 48 h of PQ exposure, mice were euthanized via the intraperitoneal injection of a high dose of sodium pentobarbital (> 150 mg/kg). Then, the mice were placed on the operating table in a supine position, and a thoracotomy was performed after skin disinfection. Blood was collected from the right ventricle with a 1 mL syringe, which was performed slowly to avoid hemolysis. Blood was then transferred to a 1.5 mL EP tube and centrifuged at 3000 r/min for 10 min at 4°C. Serum was transferred to a new 1.5 mL EP tube and stored at − 80°C. After blood collection, the lungs were flushed through the right ventricle with saline until clear fluid was drained from the lungs. Lungs were then harvested. The upper lobe of the left lung was fixed in paraformaldehyde, the lower lobe of the left lung was immediately weighed, and the right lung was stored at − 80°C.

2.1.4 Observation of lung injury through H&E staining

The upper lobe of the left lung (after fixation for at least 24 h) was removed from paraformaldehyde and dehydrated with an ascending series of graded alcohols, followed by paraffin infiltration and paraffin embedding. Tissues were sectioned into slices with a thickness of 2.5 μm. Some sections were used for H&E staining, whereas others were used for immunofluorescence. An automatic tissue stainer (Leica Autostainer) was used for H&E staining of the sections. After dehydration, slides were cleared with xylene and mounted with neutral balsam. Pathological changes were observed with a microscope (Nikon Corporation) and recorded with NIS-Element software (version 4.6). Lung injury was scored according to the method used by Mikawa et al. [20] as follows: four items were considered during scoring, including alveolar congestion, alveolar hemorrhage, infiltration of inflammatory cells, and thickening of alveolar wall, and each item was scored on a 5-point scale (0: no or extremely mild damage; 1: mild damage; 2: moderate damage; 3: severe damage; 4: extremely severe damage). The sum of the scores of each item was considered the final score for lung injury.

2.1.5 Assessment of pulmonary edema based on the wet weight/dry weight ratio of lung tissue

The lower lobe of the left lung was used for this analysis. The wet weight was first determined, and the dry weight was determined after drying the sample in an oven at 80°C for 48 h. The severity of pulmonary edema was assessed based on the calculated ratio of the wet weight/dry weight.

2.1.6 Detection of the expression of PINK1, BNIP3, and TLR9 via immunofluorescence

The automatic tissue stainer was used for dewaxing, rehydration, and antigen retrieval with the sections. The samples were cooled to room temperature naturally and then washed three times for 5 min each with PBS solution. The sections were blocked with BSA for 40 min, and the liquid on the slices was removed. Tissues were then treated with a PINK1 primary antibody (Cell Signaling Technology, 6946T), BNIP3 primary antibody (Abcam, EPR4034), and TLR9 primary antibody (Cell Signaling Technology, 13674T) at 4°C overnight. On the following day, the sections were transferred to room temperature and were washed three times for 5 min each with PBS solution. They were then incubated with a fluorescent secondary antibody (Proteintech, SA00003-2) at room temperature in the dark for 4 h and washed three times for 5 min each with PBS solution. Finally, they were incubated with DAPI solution (Solarbio, C0065) at room temperature in the dark for 5 min and washed three times for 5 min each with PBS solution. After mounting with an anti-fluorescence quenching medium (SEVEN, SI103-01), the slides were observed with a two-photon confocal microscope (Leica).

2.1.7 Observation of autophagosomes with a transmission electron microscope

Tissues were fixed with 2.5% glutaraldehyde and 1% osmic acid at 4°C for 2 h and then washed three times for 5 min each with sodium dimethacrylate. The tissues were then dehydrated with increasing concentrations of ethanol and acetone, soaked in a mixed solution of epoxy resin and acetone, and finally embedded under the microscope for sectioning and photographing.

2.1.8 Detection of serum TNF-α and IL-1β via ELISA

The serum was centrifuged at 10,000 rpm at 4°C for 10 min, and the supernatant was collected. Serum TNF-α and IL-1β levels were determined using the TNF-α detection kit (Elabscience, E-MSEL-M0002) and IL-1β detection kit (Elabscience, E-MSEL-M0003), respectively.

2.2 In vitro experiment

2.2.1 Cell culture

A549 cells were cultured in medium optimized for A549 cells (Pricella, CM-0016) in a 5% CO_2 incubator at 37°C. The medium was changed daily. When the cell density reached 60–80%, cells were passaged at a ratio of 1:3.

2.2.2 Screening of optimal PQ and MT concentrations by performing CCK8 assays

Different concentrations of PQ (0, 100, 200, 400, 600, 800, 1000, and 1200 μM) and MT (0, 400, 800, 1200, 1600, 2000, 2400, and 2800 μM) were applied to culture the cells. The CCK8 kit (Dojindo Laboratories, Inc.) was then used to screen the optimal PQ and MT concentrations, which were used as the intervention concentrations in subsequent experiments.

2.2.3 Investigation of the association between TLR9 activation and mtDNA leakage via CHIP

The cells were divided into two groups and cultured in 15 cm dishes. One group was untreated and served as the control group; the other group was treated with PQ and was referred to as the PQ group. After 48 h, purified DNA was extracted using a CHIP kit (Cell Signaling Technology, 9003) and a TLR9 primary antibody, and the levels of mtDNA bound by TLR9 were compared between the two groups. We detected mtDNA levels through the quantification of MT-CO_2 [21], using the following primers: MT-CO_2 forward primer 5'-AATCGAGTAGTACTCCCGATTG-3' and reverse primer 5'-TTCTAGGACGATGGGCATGAAA-3'.

2.2.4 Grouping of cells

Cells were divided into four groups, namely the control group (Group I), PQ group (Group II), MT + PQ group (Group III), and MT group (Group IV), which were used in subsequent experiments.

2.2.5 Observation of autophagosomes under a transmission electron microscope

The cells were washed with PBS and transferred into 1.5 mL EP tubes using a cell scraper. After centrifugation (8000 rpm, 5 min), the supernatant was discarded. Cell pellets were fixed with 2.5% glutaraldehyde and 1% osmic acid at 4°C for 2 h and then washed three times for 5 min each with sodium dimethacrylate. The cells were dehydrated with increasing concentrations of ethanol and acetone, soaked in a mixed solution of epoxy resin and acetone, and finally embedded under the microscope for sectioning and photographing.

2.2.6 Detection of mtDNA release level using PCR

The Cell Mitochondria Isolation Kit (Beyotime, C3601) was used to isolate mitochondria from cells. The remaining cell lysates were collected, and the QIAamp DNA purification mini kit (QIAGEN GmbH, 51304) was then used to extract purified DNA. Finally, the expression of MT-CO_2 was determined using the 7500 Real-time PCR System.

2.2.7 Detection of the expression of PINK1, BNIP3, TLR9, and p-P65 by western blotting

After cells were harvested with a cell scraper, a nuclear protein extraction kit (Solarbio, R0050) was used to separate cytoplasmic and nuclear proteins. Proteins in each group were separated via 10% polyacrylamide gel electrophoresis and transferred to a PVDF membrane. The membranes were blocked with 5% skim milk and then incubated with primary antibodies against PINK1, BNIP3, TLR9, p-P65 (Cell Signaling Technology, 3033S), β-actin (Cell Signaling Technology, 3700S), and TBP (Cell Signaling Technology, 44059T) at 4°C overnight. After this, the membranes were washed three times in TBST buffer (10 min each time), incubated with the secondary antibody for 2 h at room temperature, and washed three times in TBST buffer (10 min each time). Finally, an ECL kit (SEVEN, SW134-01) was used for

detection. β-Actin was used as an internal reference protein for cytoplasmic proteins, and TBP was used as an internal reference protein for nuclear proteins.

2.2.8 Detection of PINK1, BNIP3, and TLR9 by immunofluorescence

The slides on which the cells were grown were washed three times with PBS (3 min each time) in the culture plate. Next, the cells were fixed with 4% paraformaldehyde for 15 min. The slides were then washed three times with PBS (3 min each time), and excess PBS was removed using bibulous paper. After blocking with 5% fetal bovine serum at room temperature for 30 min, slides were incubated with primary antibody at 4°C overnight in a humid chamber. On the following day, slides were washed three times with PBS (3 min each time), and excess PBS was removed with bibulous paper. Then, fluorescent secondary antibodies were added, and slides were incubated in a humid chamber for 1 h at room temperature. After PBS washing, slides were incubated with DAPI at room temperature for 5 min. Slides were washed three times with PBS (3 min each time), and excess PBS was removed with bibulous paper. After mounting with an anti-fluorescence quenching medium, the slides were inspected under a fluorescent microscope.

2.2.9 Detection of TNF-α and IL-1β via ELISA

The cell supernatant was collected in a 1.5mL EP tube and centrifuged at 10,000 rpm at 4°C for 10 min. The supernatant was collected. TNF-α and IL-1β levels were determined using a TNF-α detection kit (Elabscience, E-MSEL-M0002) and IL-1β detection kit (Elabscience, E-MSEL-M0003), respectively.

2.2.10 Transfection and grouping of cells

The cells were divided into four groups, namely the control group (Group a), the PQ group (Group b), the MT + PQ + PINK1 siRNA + BNIP3 siRNA group (Group c), and the PINK1 siRNA + BNIP3 siRNA group (Group d). The transfection reagents and siRNA used in this experiment were purchased from Guangzhou RiboBio Co., Ltd, and the transfection was performed according to the instructions of the manufacturer.

2.2.11 Detection of the expression of PINK1, BNIP3, TLR9, and p-P65 in transfected cells via western blotting

After cells were harvested with a cell scraper, a nuclear protein extraction kit (Solarbio, R0050) was used to separate cytoplasmic and nuclear proteins. Proteins in each group were separated via 10% polyacrylamide gel electrophoresis and transferred to a PVDF membrane. The membranes were blocked with 5% skim milk and then incubated with primary antibodies against PINK1, BNIP3, TLR9, p-P65 (Cell Signaling Technology, 3033S), β-actin (Cell Signaling Technology, 3700S), and TBP (Cell Signaling Technology, 44059T) at 4°C overnight. Next, the membranes were washed three times in TBST buffer (10 min each time), incubated with the secondary antibody for 2 h at room temperature, and washed three times in TBST buffer (10 min each time). Finally, an ECL kit (SEVEN, SW134-01) was used for detection.

β-Actin was used as an internal reference protein for cytoplasmic proteins, and TBP was used as an internal reference protein for nuclear proteins.

2.2.12 Detection of TNF-α and IL-1β in transfected cells via ELISA

The cell supernatant was collected in a 1.5mL EP tube and centrifuged at 10,000 rpm at 4°C for 10 min. The supernatant was collected. TNF-α and IL-1β levels were determined using a TNF-α detection kit (Elabscience, E-MSEL-M0002) and IL-1β detection kit (Elabscience, E-MSEL-M0003), respectively.

2.3 Statistical analysis

GraphPad Prism 7 was used for the statistical analysis of the data. The data were presented as the mean ± standard deviation. The differences between groups were analyzed by performing one-way analysis of variance and t-test, and $P < 0.05$ was considered statistically significant.

3 Results

3.1 MT exerts a protective effect by activating mitophagy in vivo

3.1.1 MT significantly reduces pathological damage to lung tissue induced by PQ exposure

As shown in Fig. 1, alveolar walls in Groups A and D were normal, and the infiltration of inflammatory cells in the interalveolar septa was not observed. In Group B, the alveolar structure was damaged, which was accompanied by pulmonary interstitial edema and alveolar edema. The alveolar spaces had collapsed, and bloody fluid and red blood cells could be observed in some of the alveolar spaces. Compared with those in Group B, the degree of lung injury and the severity of pulmonary edema in Group C were significantly reduced.

3.1.2 MT promotes the expression of PINK1 and BNIP3, key proteins of mitophagy, and inhibits the expression of TLR9, an inflammatory protein

Immunofluorescence results are shown in Fig. 2. Compared with that in Group A, the expression of PINK1, BNIP3, and TLR9 in Group B was increased; further, the expression of PINK1 and BNIP3 was increased in Group D, with no significant change in the expression of TLR9 expression. Compared with that in Group B, the expression of PINK1 and BNIP3 in Group C was further increased, whereas the expression of TLR9 was decreased.

3.1.3 MT promotes the formation of autophagosomes to remove damaged mitochondria

As shown in Fig. 3, compared with that observed in Group A, destruction of the cell nucleus, mitochondrial swelling, and the formation of autophagosomes were observed in Group B; the cell structure in Group D was normal, and the number of autophagosomes was increased. Compared with that in Group B, the degree of nuclear damage in Group C was reduced and the number of autophagosomes was increased, which was accompanied by a decrease in the number of damaged mitochondria.

3.1.4 MT reduces the levels of inflammatory factors in serum after PQ poisoning

As shown in Fig. 4, compared with those in Group A, the levels of TNF-α and IL-1β in Group B were significantly increased and the difference was not found to be statistically significant for Group D. Compared with those in Group B, the levels of TNF-α and IL-1β in Group C were decreased, and the inflammatory response was reduced.

3.2 Specific molecular mechanism underlying the protective effect of MT, associated with mitophagy activation, based on in vitro experiments

3.2.1 Optimal concentrations of PQ and MT for intervention

As shown in Fig. 5, when cells were cultured with different concentrations of PQ, cell viability gradually decreased with an increase in the PQ concentration. When the PQ concentration was 600 μM, the survival rate of cells was close to 50%, suggesting that this concentration was the half-maximal inhibitory concentration. Similarly, changes in cell viability when cells were treated with different concentrations of MT were assessed, and no significant difference in cell viability was observed, indicating that MT had no obvious cytotoxicity. In addition, cells exposed to PQ (600 μM) were treated with different concentrations of MT; we found that when the MT concentration was 1200 μM, the highest cell viability was achieved. Therefore, we selected 600 μM and 1200 μM as the optimal concentrations of PQ and MT, respectively, for subsequent intervention.

3.2.2 Association between mtDNA leakage and TLR9 hyperactivation based on CHIP

By quantifying MT-CO_2, the level of mtDNA that led to TLR9 activation could be obtained, as shown in Fig. 6. After PQ intervention, the content of MT-CO_2 in the extracted and purified DNA was increased significantly compared with that in the control group. This indicates that the activation of TLR9 is closely related to mtDNA leakage during PQ poisoning.

3.2.3 Autophagosomes observed using electron microscopy

As shown in Fig. 7, the findings were consistent with the in vivo study. Compared with that observed in Group I, destruction of the cell nucleus, mitochondrial swelling, and formation of autophagosomes were observed in Group II; the cell structure in Group IV was normal, and the number of autophagosomes was increased. Compared with those in Group II, the degree of nuclear damage in Group III was reduced and the number of autophagosomes was increased, which was accompanied by a decrease in the number of damaged mitochondria.

3.2.4 MT reduces mtDNA leakage into the cytoplasm

As shown in Fig. 8, compared with that in Group , the MT-CO_2 level in Group was increased; no significant difference was observed in Group . Compared with that in Group , the level of MT-CO_2 in Group was decreased, suggesting that mtDNA leakage into the cytoplasm was decreased after MT intervention.

3.2.5 MT upregulates the expression of key proteins involved in mitophagy and reduces the TLR9-mediated inflammatory response

Through western blotting (Fig. 9), immunofluorescence (Fig. 10), and ELISA (Fig. 11), we observed that compared with that in Group , the expression of PINK1, BNIP3, and downstream inflammatory proteins of TLR9 in Group was increased, and the release of inflammatory factors was enhanced, indicating that PQ exposure resulted in inflammation and that mitophagy was used by the body as a self-protection strategy. The expression of PINK1 and BNIP3 was increased in Group IV, without a significant change in the inflammatory response mediated by TLR9, indicating that MT promoted the expression of key proteins involved in mitophagy. Compared with that in Group , the expression of PINK1 and BNIP3 in Group was further increased, whereas the inflammatory response mediated by TLR9 was reduced, suggesting that MT reduced the inflammatory response mediated by TLR9 after PQ poisoning through the activation of mitophagy.

3.2.6 PINK1 and BNIP3 downregulation abrogates the suppressive effect of MT on the inflammatory response mediated by PQ exposure

As shown in Figs. 12–14, compared with those in Group a, the expression of PINK1 and BNIP3 (Fig. 12), mtDNA levels (Fig. 13), and the release of inflammatory factors (Fig. 14) were increased in Group b; no significant expression of PINK1 and BNIP3 was observed in Group d, indicating that transfection was successful. Compared with those in Group b, no significant expression of PINK1 and BNIP3 was observed in Group c, and the inflammatory response mediated by TLR9 was aggravated, suggesting that the protective effect of MT was abrogated. This result further proves that MT exerts its protective effect by promoting the expression of PINK1 and BNIP3, verifying our conjecture.

4 Discussion

PQ, a widely used herbicide, is highly toxic and extremely harmful to human health, and currently, no effective treatment exists for PQ poisoning. As PQ is structurally similar to polyamines, after it enters the human body, alveolar cells will actively transport it into the alveolar epithelial cells through the polyamine transport system. PQ then disrupts the mitochondrial electron transport chain, which causes structural abnormalities in the mitochondria, resulting in mtDNA leakage into the cytoplasm. As fully unmethylated DNA, mtDNA is probably recognized by TLR9, activating downstream inflammatory pathways, causing the release of TNF-α and IL-1β, and thereby resulting in lung injury. As a self-protection mechanism of cells, mitophagy can maintain the stability of the intracellular environment by removing damaged mitochondria. However, MT can promote the expression of PINK1 and BNIP3, which are key proteins involved in mitophagy. Therefore, we speculate that the administration of MT to cells exposed to PQ can result in the activation of mitophagy to remove damaged mitochondria and reduce the leakage of mtDNA. In this study, we first explored the roles of MT and mitophagy in the inflammatory response induced by PQ exposure by performing an in vivo study. The results generally showed that MT could reduce the infiltration of inflammatory cells and pulmonary fibrosis induced by PQ exposure and significantly reduce the levels of inflammatory factors in serum, demonstrating the protective effect of MT. In addition, we also found that after PQ exposure, the expression of PINK1 and BNIP3, key mitophagy-associated proteins, was increased, and when observed under an electron microscope, the number of autophagosomes was also increased; however, after MT intervention, mitophagy was further activated, which was accompanied by a smaller number of damaged mitochondria. This result indicates that mitophagy can be used by the body as a self-protection mechanism to remove damaged mitochondria and that MT can promote this process. Based on the in vitro experiment, we found that mtDNA leakage could induce the hyperactivation of TLR9, consequently activating downstream inflammatory pathways; after MT intervention, mitophagy was further upregulated, and some mtDNA that leaked into the cytoplasm was removed, reducing the inflammatory response mediated by TLR9, the levels of TNF-α and IL-1β, and therefore, the acute inflammatory response caused by PQ exposure. To further verify that MT exerts a protective effect by affecting mitophagy, we treated A549 cells exposed to PQ with MT after inhibiting the expression of PINK1 and BNIP3. The results showed that when the expression of PINK1 and BNIP3 were inhibited, MT intervention could not reduce the inflammatory response induced by PQ exposure, which further verifies our hypothesis that MT reduces PQ-induced acute lung injury by affecting mitophagy.

Through this study, we hope to provide guidance for the clinical treatment of PQ poisoning to reduce associated mortality. However, several questions remain to be addressed by further research, such as whether the process of mtDNA leakage is regulated by a specific protein and the molecular mechanism underlying this regulation.

Declarations

1 Conflict of Interest

The authors declare that the research was conducted in the absence of any commercial or financial relationships that could be construed as a potential conflict of interest.

2 Author Contributions

YY and HS contributed to conception and design of the study. YYwrote the first draft of the manuscript. All authors contributed to the article and approved the submitted version.

3 Funding

This study was funded by the Foundation of LiaoningEducation Department (JCZR2020014), the LiaoningProvince Key R&D Program (grant no. 2020JH2/10300141) and the 345 Talent Project of Shengjing Hospital.

References

1. Tong, T., et al., *Paraquat exposure induces Parkinsonism by altering lipid profile and evoking neuroinflammation in the midbrain*. Environ Int, 2022. **169**: p. 107512.
2. Xia, J., et al., *Study of paraquat-induced pulmonary fibrosis using biomimetic micro-lung chips*. Biofabrication, 2022.
3. Usher, J.L., et al., *Parkin drives pS65-Ub turnover independently of canonical autophagy in Drosophila*. EMBO Rep, 2022: p. e202153552.
4. Vellingiri, B., et al., *Neurotoxicity of pesticides - A link to neurodegeneration*. Ecotoxicol Environ Saf, 2022. **243**: p. 113972.
5. Wijaya, L.S., et al., *Stimulation of de novo glutathione synthesis by nitrofurantoin for enhanced resilience of hepatocytes*. Cell Biol Toxicol, 2022. **38**(5): p. 847–864.
6. Cui, Y., et al., *Arenaria kansuensis attenuates pulmonary fibrosis in mice via the activation of Nrf2 pathway and the inhibition of NF-kB/TGF-beta1/Smad2/3 pathway*. Phytother Res, 2021. **35**(2): p. 974–986.
7. Deng, G., L. Li, and Y. Ouyang, *Modeling paraquat-induced lung fibrosis in C. elegans reveals KRIT1 as a key regulator of collagen gene transcription*. Aging (Albany NY), 2021. **13**(3): p. 4452–4467.
8. da Silva-Junior, E.B., et al., *Pulmonary Fibrosis and Hypereosinophilia in TLR9(-/-) Mice Infected by Cryptococcus gattii*. Pathogens, 2022. **11**(9).
9. Miyazaki, D., et al., *Role Played by Receptors for Advanced Glycosylation End Products in Corneal Endothelial Cells after HSV-1 Infection*. Int J Mol Sci, 2021. **22**(11).
10. Valentin, R., et al., *Sequence-dependent inhibition of cGAS and TLR9 DNA sensing by 2'-O-methyl gapmer oligonucleotides*. Nucleic Acids Res, 2021. **49**(11): p. 6082–6099.

11. Praharaj, P.P., B.S. Patro, and S.K. Bhutia, *Dysregulation of mitophagy and mitochondrial homeostasis in cancer stem cells: Novel mechanism for anti-cancer stem cell-targeted cancer therapy*. Br J Pharmacol, 2022. **179**(22): p. 5015–5035.
12. Song, C., et al., *Mitophagy: A novel perspective for insighting into cancer and cancer treatment*. Cell Prolif, 2022: p. e13327.
13. Imran, M., et al., *Melatonin and nitric oxide: Dual players inhibiting hazardous metal toxicity in soybean plants via molecular and antioxidant signaling cascades*. Chemosphere, 2022. **308**(Pt 3): p. 136575.
14. Luchetti, F., et al., *Melatonin, tunneling nanotubes, mesenchymal cells, and tissue regeneration*. Neural Regen Res, 2023. **18**(4): p. 760–762.
15. Su, Q., et al., *Agomelatine: a potential novel approach for the treatment of memory disorder in neurodegenerative disease*. Neural Regen Res, 2023. **18**(4): p. 727–733.
16. Wang, Z., et al., *Melatonin maintained higher contents of unsaturated fatty acid and cell membrane structure integrity in banana peel and alleviated postharvest chilling injury*. Food Chem, 2022. **397**: p. 133836.
17. Tang, H., et al., *Melatonin alleviates renal injury by activating mitophagy in diabetic nephropathy*. Front Endocrinol (Lausanne), 2022. **13**: p. 889729.
18. Yoon, Y.M., et al., *Melatonin Treatment Improves Renal Fibrosis via miR-4516/SIAH3/PINK1 Axis*. Cells, 2021. **10**(7).
19. Zhou, H., et al., *Effects of melatonin on fatty liver disease: The role of NR4A1/DNA-PKcs/p53 pathway, mitochondrial fission, and mitophagy*. J Pineal Res, 2018. **64**(1).
20. Mikawa, K., et al., *ONO-1714, a nitric oxide synthase inhibitor, attenuates endotoxin-induced acute lung injury in rabbits*. Anesth Analg, 2003. **97**(6): p. 1751–1755.
21. Willemsen, J., et al., *TNF leads to mtDNA release and cGAS/STING-dependent interferon responses that support inflammatory arthritis*. Cell Rep, 2021. **37**(6): p. 109977.

Figures

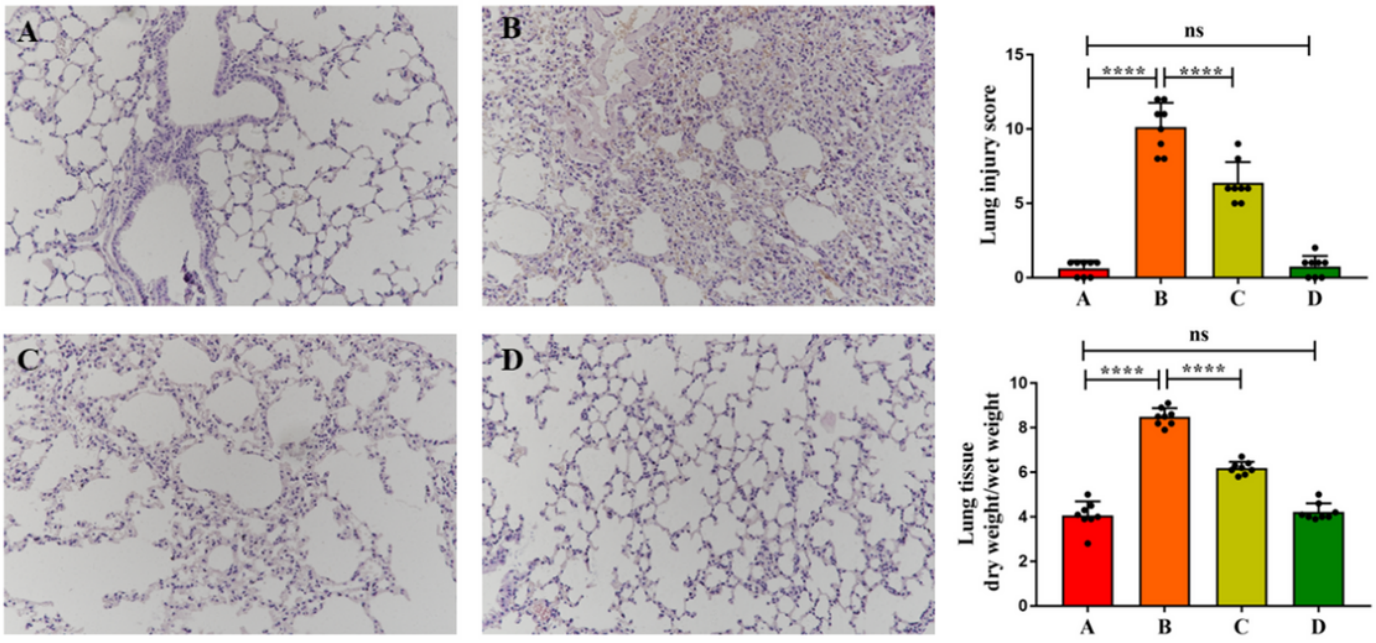

Figure 1

Melatonin (MT) significantly reduces pathological damage to lung tissue caused by paraquat (PQ) exposure. (A) normal control, (B) PQ group, (C) MT+PQ group, and (D) MT group. ****: P<0.0001, ns: statistically non-significant (P>0.05).

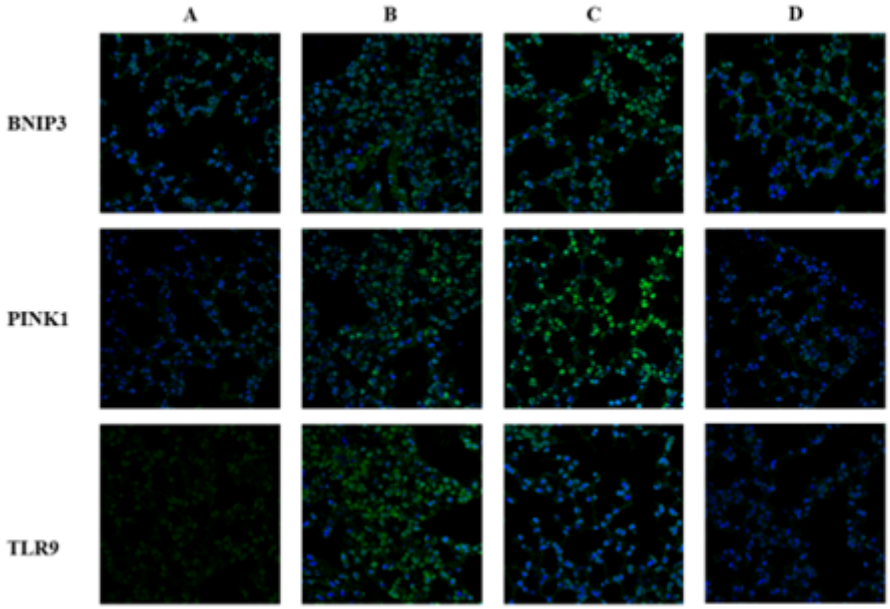

Figure 2

Melatonin (MT) promotes the expression of PINK1 and BNIP3, which are key proteins involved in mitophagy, and inhibits the expression of TLR9, an inflammatory protein.

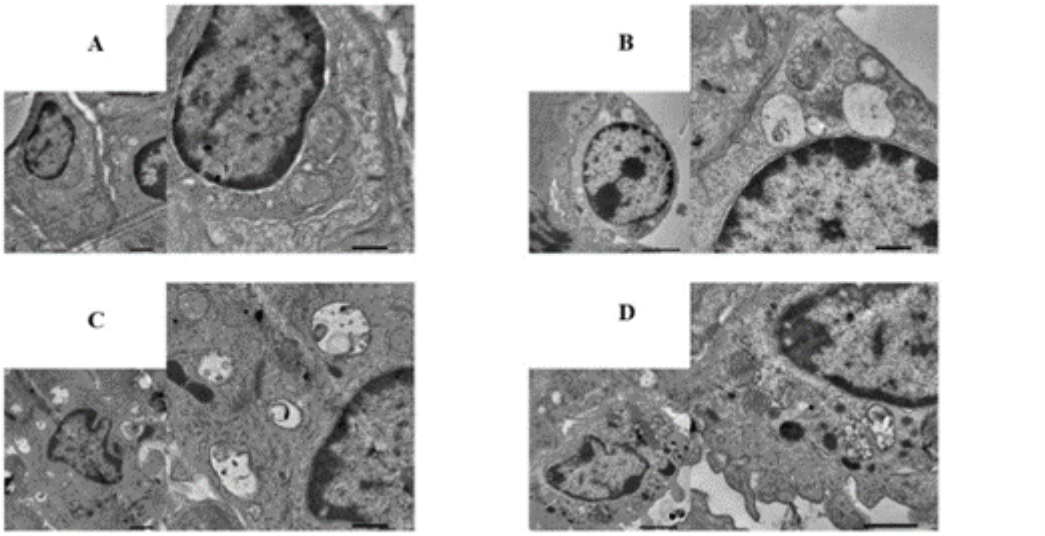

Figure 3

Melatonin (MT) promotes the formation of autophagosomes to remove damaged mitochondria.

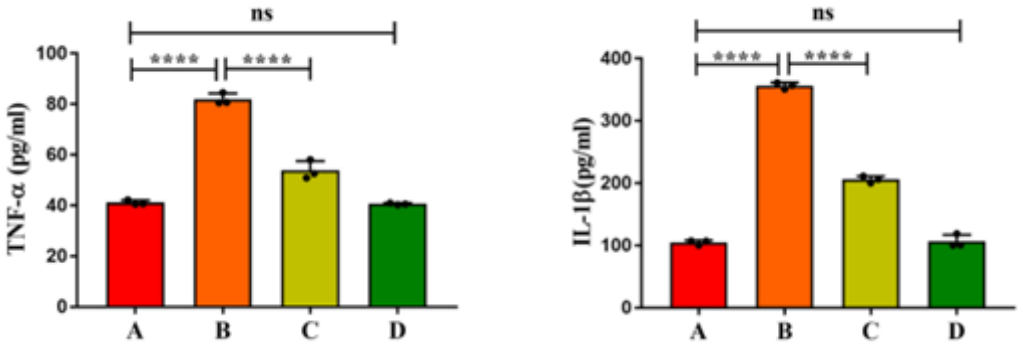

Figure 4

Melatonin (MT) reduces the levels of inflammatory factors in serum after paraquat (PQ) poisoning. (A) control group, (B) PQ group, (C) MT+PQ group, and (D) MT group. ****: P<0.0001, ns: statistically non-significant (P>0.05).

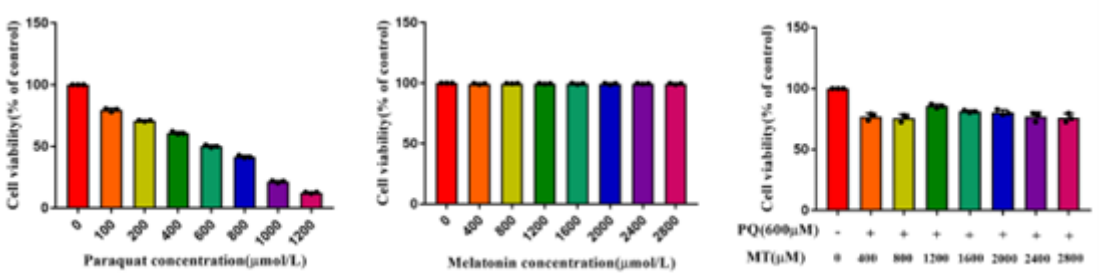

Figure 5

Screening of optimal concentrations of paraquat (PQ) and melatonin (MT) for intervention based on CCK8 assays.

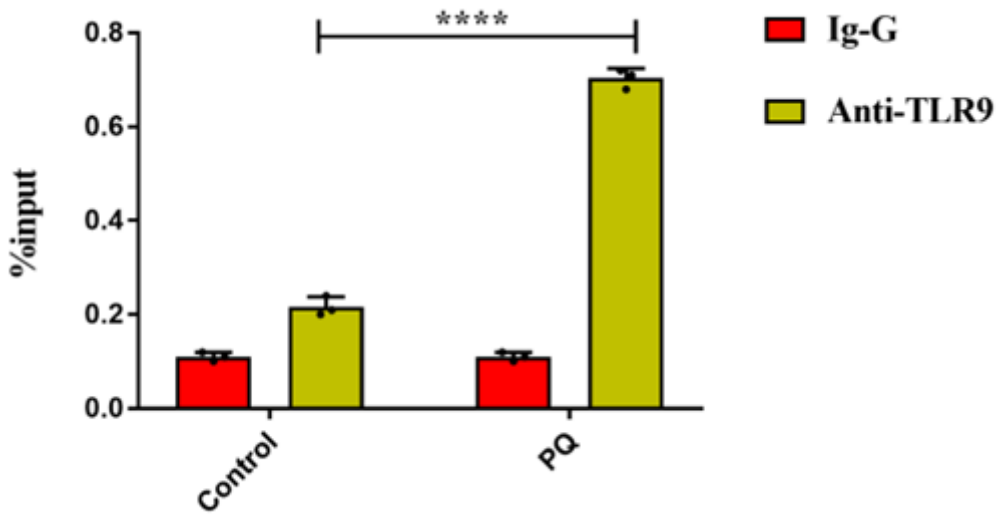

Figure 6

Mitochondrial DNA (mtDNA) leakage results in TLR9 hyperactivation. ****: P<0.0001. PQ, paraquat.

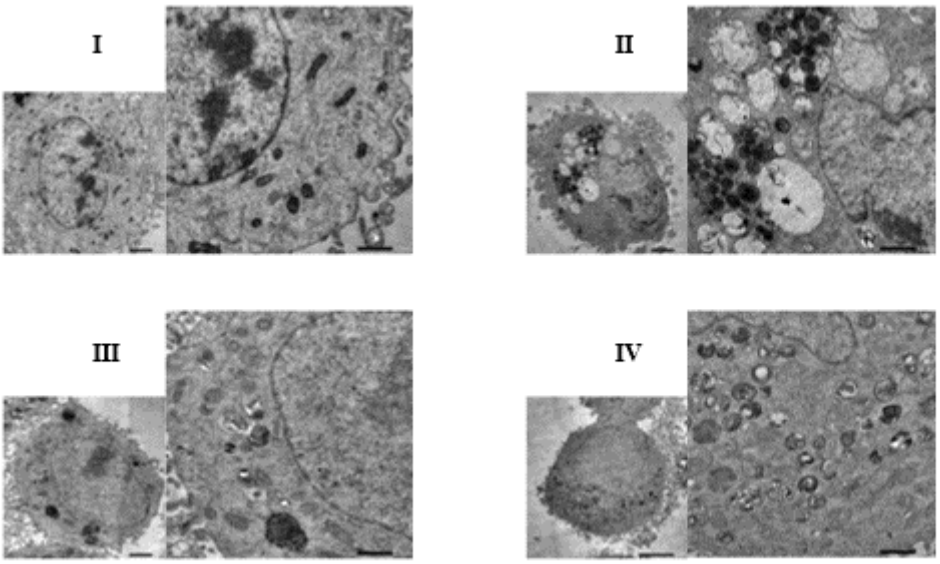

Figure 7

Electron microscopy of autophagosomes. : normal control, : PQ group, : MT+PQ group, and : MT group.

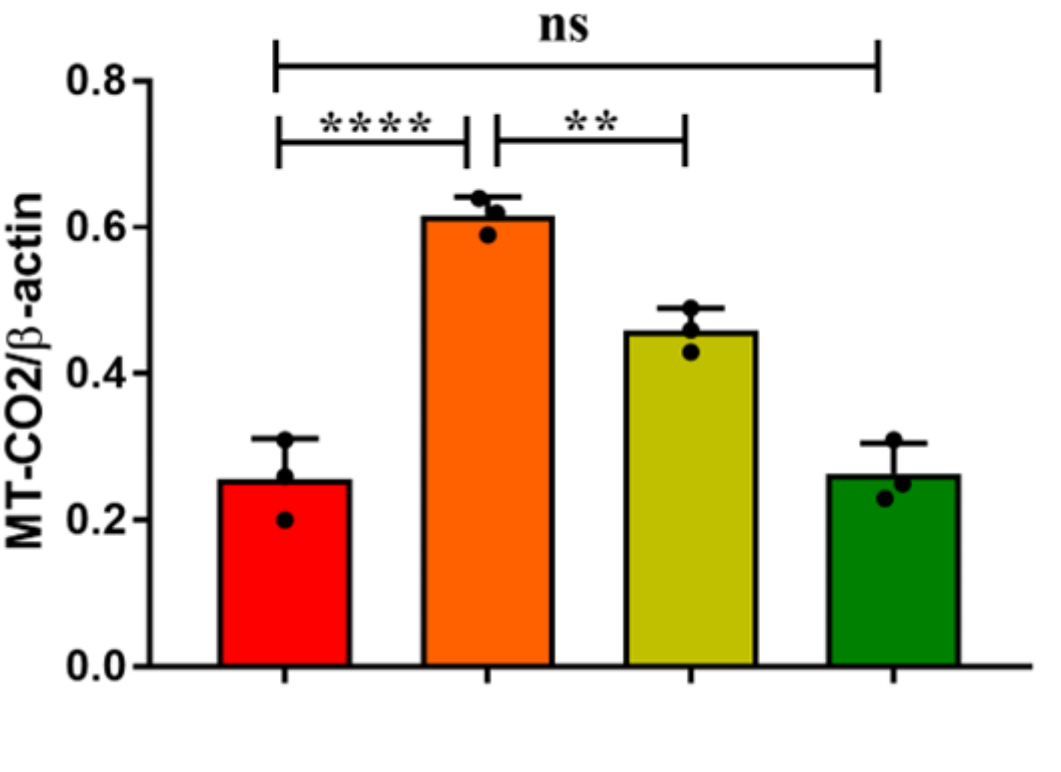

Figure 8

Melatonin (MT) reduces mitochondrial DNA (mtDNA) leakage into the cytoplasm. : normal control, : PQ group, : MT+PQ group, and : MT group. ****: P<0.0001, ***: P<0.001, **: P<0.05, ns: statistically non-significant (P>0.05). PQ, paraquat.

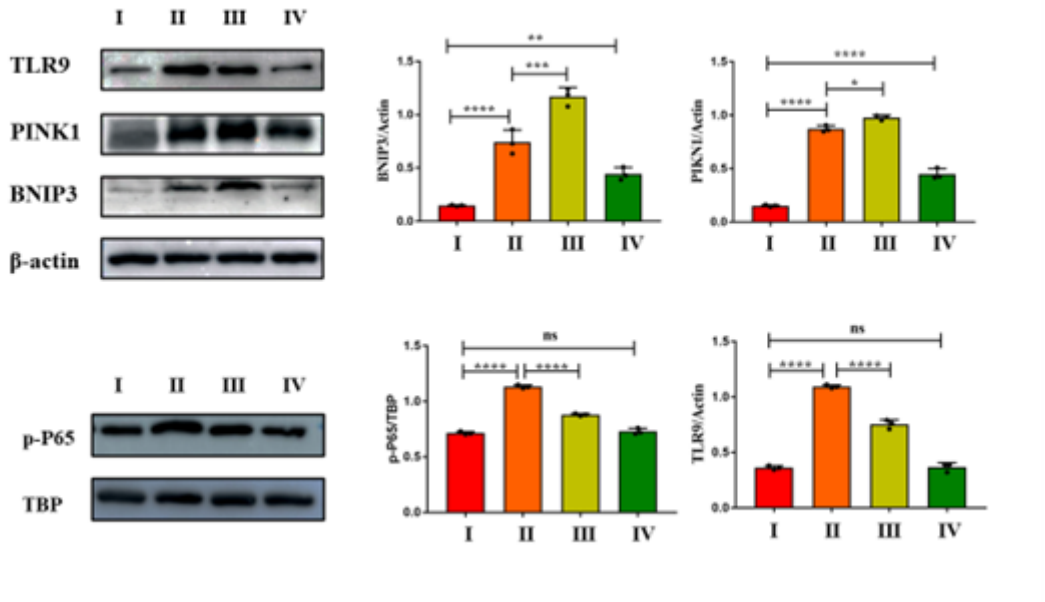

Figure 9

Detection of expression of PINK1, BNIP3, p-P65, and TLR9 via western blotting. : normal control, : PQ group, : MT+PQ group, and : MT group. ****: P<0.0001, ***: P<0.001, **: P<0.01, *: P<0.05, ns: statistically non-significant (P > 0.05). MT, melatonin; PQ, paraquat.

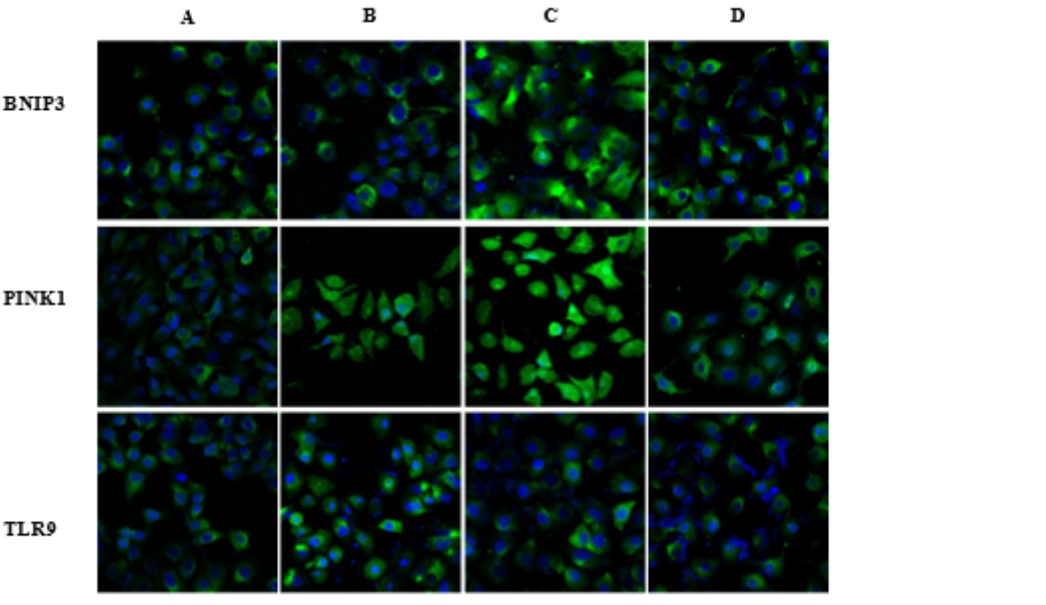

Figure 10

Detection of expression of PINK1, BNIP3, and TLR9 via immunofluorescence.

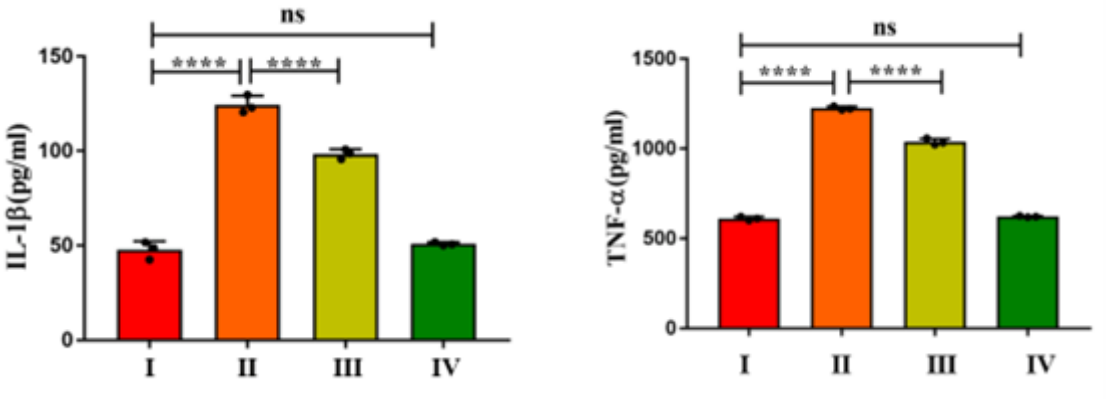

Figure 11

Detection of TNF-α and IL-1β via ELISA. : normal control, : PQ group, : MT+PQ group, and : MT group. ****: P<0.0001, ns: statistically non-significant (P>0.05). PQ, paraquat; MT, melatonin.

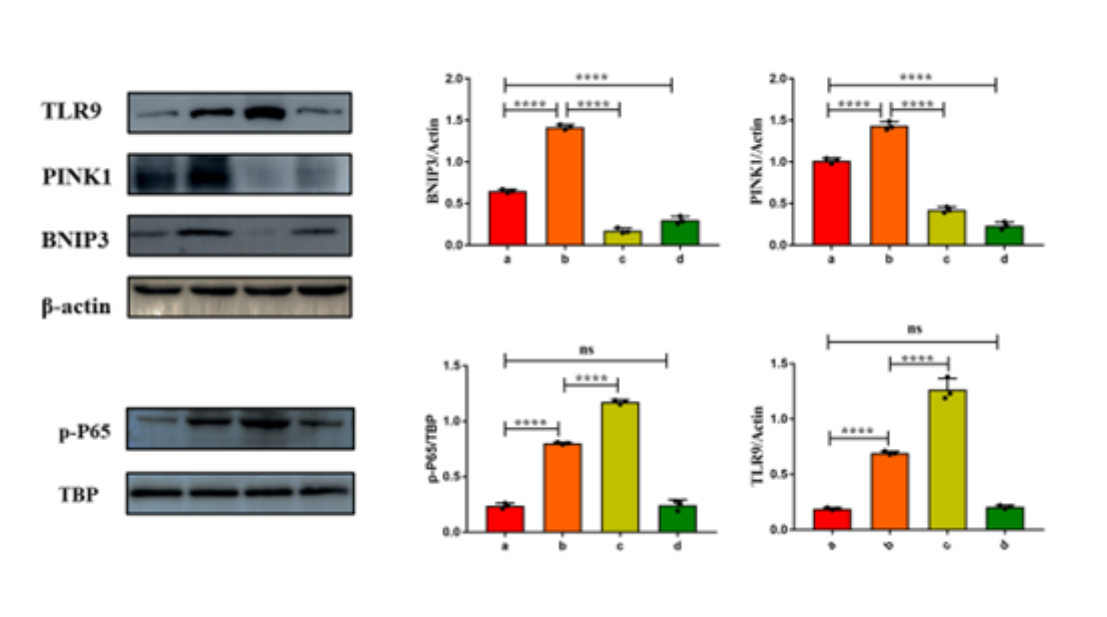

Figure 12

Detection of expression of PINK1, BNIP3, p-P65, and TLR9 via western blotting. (A) normal control, (B) PQ group,(C) MT+PQ+PINK1 siRNA+BNIP3 siRNA group, and (D) PINK1 siRNA+BNIP3 siRNA group. ****: P<0.0001, ns: statistically non-significant (P>0.05). PQ, paraquat; MT, melatonin.

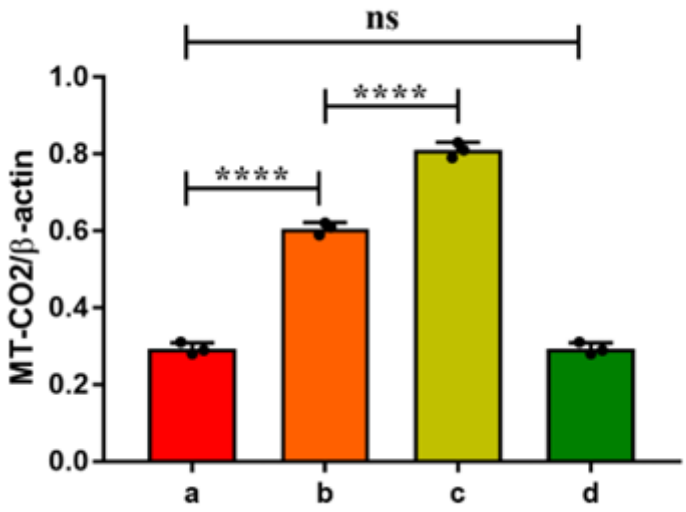

Figure 13

PINK1 and BNIP3 downregulation abrogates the inhibitory effect of melatonin (MT) on mitochondrial DNA (mtDNA) leakage induced by paraquat (PQ) exposure. (A) normal control, (B) PQ group, (C) MT+PQ+PINK1 siRNA+BNIP3 siRNA group, and (D) PINK1 siRNA+BNIP3 siRNA group. ****: P<0.0001, ns: statistically non-significant (P>0.05).

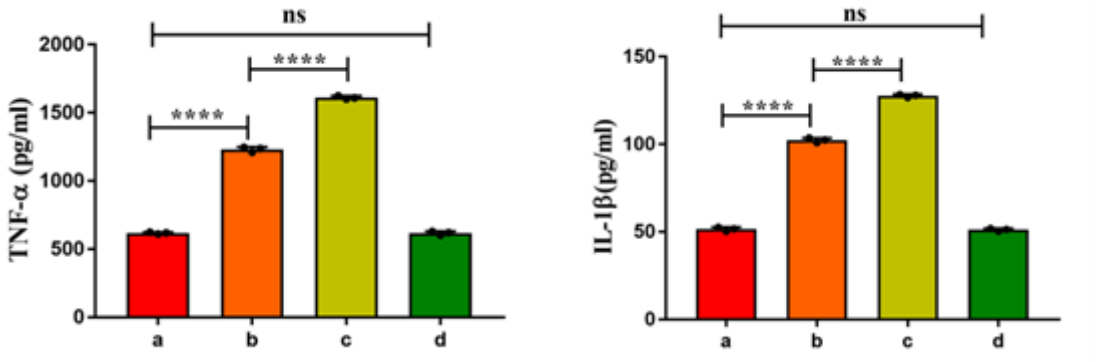

Figure 14

PINK1 and BNIP3 downregulation suppresses the ability of melatonin (MT) to reduce the release of inflammatory factors induced by paraquat (PQ) exposure. (A) normal control, (B) PQ group, (C) MT+PQ+PINK1 siRNA+BNIP3 siRNA group, and (D) PINK1 siRNA+BNIP3 siRNA group. ****: P<0.0001, ns: statistically non-significant (P>0.05).